SAND2017-2145C

10th U. S. National Combustion Meeting
Organized by the Eastern States Section of the Combustion Institute
April 23-26, 2017
College Park, Maryland

Mass-Loss Measurements on Solid Materials after Pulsed Radiant Heating at High Heat Flux

Jeffrey D. Engerer[1], Alexander L. Brown[1,], Joshua M. Christian[2]*

[1]Fire Science and Technology, Sandia National Laboratories, P.O. Box 5800
Albuquerque, NM, 87185-1135, USA
[2]Concentrating Solar Technologies, Sandia National Laboratories, P.O. Box 5800
Albuquerque, NM, 87185-1127, USA

[*]Corresponding Author Email: albrown@sandia.gov

Abstract: When exposed to a strong radiant heat source (>1,000 kW/m^2), combustible materials pyrolyze and ignite under certain conditions. Studies of this nature are scarce, yet important for some applications. Pyrolysis models derived at lower flux conditions do not necessarily extrapolate well to high-heat-flux conditions. The material response is determined by a complex interplay of thermal and chemical transport phenomena, which are often difficult to model. To obtain model validation data at high-heat-flux conditions (up to 2500 kW/m^2), experiments on a variety of organic and engineered materials were performed at the National Solar Thermal Test Facility at Sandia National Laboratories. Mass loss during the short duration (2–4 sec) heat pulse was determined using the pre- and post-test weight. The mass-loss data were fairly linear in the fluence range of 200–6000 kJ/m^2. When divided into subsets based on material types, the mass loss was similar at the peak flux/fluence condition for engineered polymers (≈1 g) and organic materials (≈2.5 g), although some exceptions exist (PMMA, dry pine needles). Statistical correlations were generated and used to evaluate the significance of the observed trends. These results contribute to the validation data for simulating fires and ignition resulting from very high incident heat flux.

Keywords: Fire, Radiant Heating, High Heat Flux, Mass Loss, Pyrolysis

1. Introduction

The majority of fire scenarios concern a solid reacting material pyrolyzing under the effects of a heat source, whether radiative or convective. In a typical fire environment, the heat flux incident on such a surface can reach values on the order of 100 kW/m^2 [1]. While data below this limit are available for a variety of materials, limited data are available for heat flux environments reaching and exceeding 1,000 kW/m^2.

Historical data on materials exposed to very high heat flux (>1,000 kW/m^2) were predominately motivated by the high-intensity pulse (~1 sec) of thermal radiation produced by nuclear airbursts. These experiments were conducted on a variety of common materials found in urban and rural environments and provided data relevant to ignition and fire spread following a detonation. Compiling available data, Glasstone and Dolan [2] presented a table of ignition times, dependent on the yield of the weapon. Qualitative descriptions were included about the material response, such as flames, embrittlement, or melting.

Working in the same heat-flux regime, Martin produced an extensive dataset for paper exposed to thermal radiation with a focus on alpha-cellulose darkened with carbon black [3, 4]. These data were used to compile a map identifying ignition based on non-dimensional flux and fluence parameters [5] and contributed to the reported ignition thresholds in Glasstone and Dolan [2, 6]. The rate of mass loss peaked around the time of ignition and was constant thereafter [5].

The data included in the present study were obtained from an ongoing set of experiments reexamining the ignition thresholds and material response at very high heat flux. The mass-loss data indicate the extent and rate of pyrolysis during radiative heating and are useful for validating fire models of solid reacting materials, yielding an estimation of the pyrolysis-gas source term. Additionally, mass loss is a quantitative description of the material response, contributing to the mostly qualitative historical data on materials exposed to nuclear airbursts.

2. Experimental Setup and Methods

A variety of materials, including predominantly lignocellulosic and polymer materials, were exposed to the following nominal fluence levels: 200, 500, 2,000, 4,000, and 6,000 kJ/m^2. To obtain such high fluence over short (2–4 s) pulses, the experiments were conducted using the solar furnace at the National Solar Thermal Test Facility (NSTTF) at Sandia National Laboratories in Albuquerque, New Mexico. The solar furnace concentrates sunlight up to approximately 6,000 kW/m^2 over a circle with a diameter of roughly 6 cm. A heliostat uses flat mirrors with a total reflective surface area of 54.76 m^2 to reflect the sunlight through an attenuator (to control the amount of power) onto a large, reflective parabolic dish. The parabolic dish concentrates the sunlight with 228 individually aligned mirrors and has an overall diameter of 6.8 m with a focal length of 4.1 m. The mirrors are composed of silvered, low-iron glass structure; consequently, the spectral composition is similar to solar spectrum with attenuation in the UV and beyond 1 micron.

The irradiation during each experiment varied dynamically with the prolonged actuation of the attenuator. The time-varying heat flux was evaluated in separate measurements taken immediately before and after the experiment. A Kendall radiometer determined the peak heat flux reached during the experiment. A Gardon-style heat-flux gauge characterized the transient heating profile.

Figure 1a displays the flux and fluence recorded by the heat-flux gauge for a representative shot at a nominal fluence of 6,000 kJ/m^2. The objective was to reach the target fluence in the shortest amount of time; the shape of the curve was limited by the responsiveness of the attenuator system. As a result, the time spent ramping to and holding at the peak do not change proportionally. Low-fluence shots spend a greater percentage of time at the peak, while high-fluence shots spend more time ramping, as shown in Figure 1b.

Two main factors were identified as affecting the accuracy of the heat-flux data for these tests. First, the Kendall radiometer had an accuracy of ±2%. Second, the radiometer and heat-flux gauge data were not recorded during the exposure of the sample; consequently, the heat flux incident on the sample was not perfectly known due to random variations in system performance and solar irradiance. Accounting for these sources of error, the accuracy of the reported flux and fluence values is ±4.3% (90% confidence).

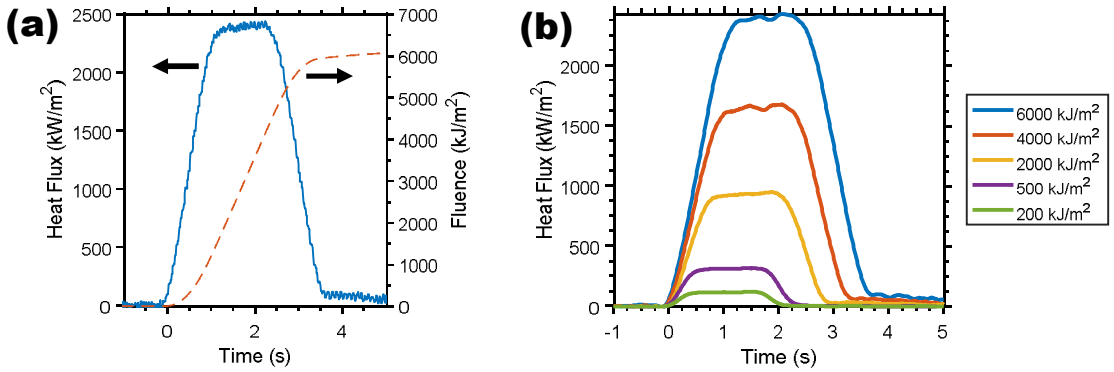

Figure 1: Examples of temporal heat-flux profiles produced by the solar furnace as recorded by the heat-flux gauge. (a) Dynamic flux and fluence at a nominal flux of 6,000 kJ/m^2. (b) Transient flux profile for a series of experiments performed at various nominal fluence levels.

The reported flux and fluence were measured at the center of the solar beam where irradiation was the most intense; however, the solar furnace did not produce a spatially uniform flux with a well-defined spot diameter. The radially varying concentration was quantified in a previous study [7]. The spatially and temporally dependent flux is expressed in the following form:

$$q''(t,r) = \frac{q_o''(t)}{1+\exp\left(C\left(\frac{R_0}{R_1}r\right)^D - B\right)} \quad (1)$$

where $q_o''(t)$ is the peak flux at the center of the spot, R_0 is the projected beam radius at the focal plane, R_1 is the projected beam radius outside of the focal plane, and B, C, and D are coefficients determined by the slope error of the parabolic dish. The spatial distribution produced by the solar furnace was best characterized using a slope error of 3 milliradians (B=6.662, C=27.7, D=0.401) and assuming the ratio of the projected beam radii is $R_0/R_1 = 1.34$ [7].

A variety of combustible materials were selected due to their ubiquity in urban and rural environments. Three materials, namely cellulose, PMMA, and polystyrene, were prospects for high-fidelity-model validation because they are well-studied and characterized. The remainder of the tests were conducted to explore material response and compare with historical data. Table 1 compiles the test conditions for each material.

Table 1: Prescribed experimental conditions. Description includes sample thickness.

Material	Description	Samples	Nom. Fluence (MJ/m^2)
Cellulose	compressed, 51 µm, α-cellulose powder	5	6
PMMA	3.12 mm; opaque, black sheet	5	6
Polystyrene	3.12 mm; high-impact, white sheet	5	6
Paper	blue-lined notebook paper, 70 sheets	5	0.2–6
Rubber/Tire	Tempest Touring SR P205/75R15	5	0.5–6
Fabric	0.91 mm; olive green, flame and water proof	5	0.2–6
Polycarbonate Roofing	1.69 mm; gray, foamed, corrugated	2	6
Wood Shingles	6–12 mm; cedar shingles, weathered	2	6
Dry Needles	collected under pine tree	3	6
Green Needles	from live pine tree, less than one day old	3	6
Wood	19 mm; pine lumber	2	6
Epoxy/Fiber Composite	3.12 mm; fiberglass-reinforced polyester	2	6

During the experiment, data were primarily obtained by two video cameras and a thermocouple on the back of the samples. In addition, mass, photographs, and 3D scans were taken before and after testing. The scale had a resolution of 0.1 g, which was comparable to the net mass-loss for some materials. Thermocouple data were unreliable and are excluded from this report. The images provided qualitative information about charring, deformation, and approximate crater size.

3. Results

The videos, photographs, and 3D scans provided valuable information on the material response; however, the data are not suited for a condensed, written report. Instead, key points are summarized here. All materials exhibited a strong response to the highest fluence level (6,000 kJ/m^2). The visible response at the lowest flux conditions was either negligible (200 kJ/m^2) or relatively small (500 kJ/m^2). In general, the area affected on the sample was comparable to the size of the solar beam, approximately 6 cm in diameter. Dry pine needles were an exceptional case; each sample smoldered for approximately 30 minutes, flaring up occasionally, until the needles were entirely consumed.

The samples, other than dry needles, only exhibited flaming ignition during the heat pulse, if at all. Only three samples, paper, fabric, and dry needles, were clearly flaming based on the videos, as evidenced by flame luminescence. Green needles and PMMA displayed no sign of ignition. For the rest of the materials, the presence or absence of a flame could not be determined conclusively. In general, the reflected light from the exposed sample was too intense to distinguish flame luminescence. Additional flame-detection methods are planned for future trials.

Relying on the data obtained by the 3D scanner, the craters formed in the samples were generally up to 2 mm deep at the highest fluence condition (6,000 kJ/m^2). A notable exception was PMMA, for which the crater had penetrated through the 3.12 mm sample for three of the five tests. The PMMA samples also developed the widest crater from the heat pulse (8–9 cm diameter).

Mass-loss data are presented graphically in Figure 2(a) for lignocellulosic materials. Most experiments were performed at a nominal fluence of 6,000 kJ/m^2; the fluence was only intentionally varied for the fabric and paper samples. Despite recording net mass loss, the visible response of the following samples was negligible: Fabric at 200 kJ/m^2 and Paper at both 210 and 400 kJ/m^2. The mass-loss data for cellulose, ranging between 1.6 g and 3.0 g, were scattered relative to other materials, perhaps reflecting variabilities in the sample preparation.

Mass-loss data for the engineered polymers are included in Figure 3(b). In this data set, the fluence was only varied for the tire samples; the other materials were exclusively tested at 6,000 kJ/m^2. Consistent with previous comments on the visual response, PMMA lost significantly (roughly 5x) more mass than the other engineered polymers. The mass-loss data for the rest of the polymers are grouped around 1 g at the highest fluence. When comparing repeats of the same materials, the mass-loss data for polymer materials exhibit less variation than that of the lignocellulosic materials.

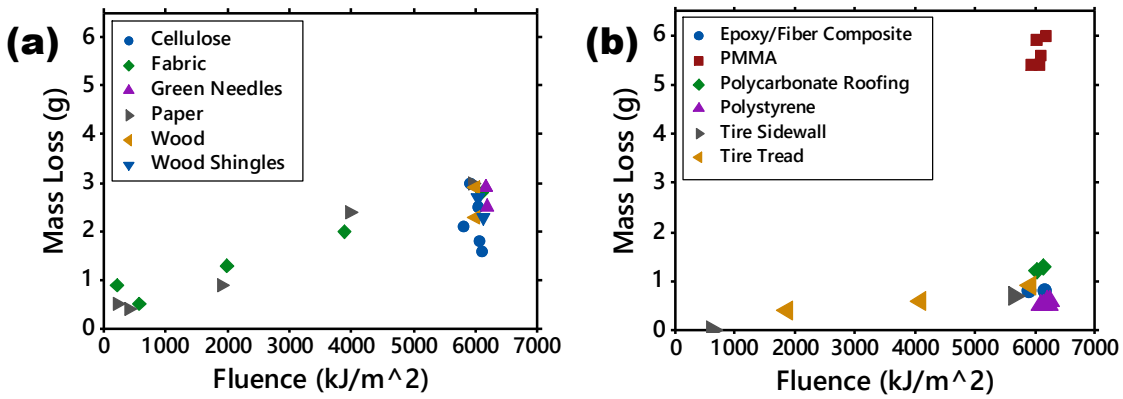

Figure 2. Mass loss data for (a) lignocellulosic materials and (b) engineered polymers.

4. Discussion

The mass-loss data for the lignocellulosic materials are appreciable at low fluence, yet the samples did not respond visibly. This fact, combined with the data scatter, indicate the mass-loss measurements may have been influenced by variations in sample water content. Humidity was not controlled during the storage or testing of these samples.

When evaluated within their groupings, the mass-loss data from the organic and polymer materials were similar, despite wide variation of the visible response to the incident heat. Operating at extreme heat flux might lessen the impact of otherwise important material properties. For example, the amount of heat from the flame returning to a burning solid material is typically in the range of 10–100 kW/m^2 [8], far lower than the radiative heat flux reached in these experiments (approximately 2500 kW/m^2).

The variation of mass-loss with fluence was examined for statistical significance using a backwards-elimination stepwise regression, starting with a quadratic model and dropping terms with p-values greater than 0.1. Quadratic terms were eliminated in all cases while linear terms were maintained. Assuming a linear correlation ($\Delta m = A + BQ_0''$), terms for mass loss, Δm (g), dependent on fluence, Q_0'' (kJ/m^2), are included in Table 2 along with 90% confidence intervals. The intercept was insignificant for paper (p-value of 0.20) and tire (p-value of 0.92).

Table 2: Terms in correlation of mass loss (g) with fluence (kJ/m^2) with 90% confidence intervals.

Material	Intercept (A)	Slope (B)
Fabric	5.7×10^{-1} ($\pm 61\%$)	3.6×10^{-4} ($\pm 29\%$)
Paper	N/A	5.3×10^{-4} ($\pm 15\%$)
Tire	N/A	1.4×10^{-4} ($\pm 15\%$)

Due to the non-uniform, radial distribution of heat flux produced by the solar furnace, the irradiated area of the sample is not easily defined. This is problematic because the mass flux is a more relevant property for analysis than the net mass loss. The net mass flux cannot be easily resolved spatially; therefore, a relevant approximation of the area must be made. In some cases, the size of the visibly-affected area in the post-test image can be used; however, in many cases the edge of the crater is not distinct. More universally, the area can be approximated as the

equivalent spot size at peak flux that delivers the same net energy. The effective spot area, A_{eff}, is calculated as:

$$A_{eff} = \frac{\int_{t=0}^{t_f} \int_{r=0}^{\infty} q''(r,t) dr dt}{\int_{t=0}^{t_f} q_0''(t)\, dt} \quad (2)$$

where t_f is the duration of the heat pulse and $q''(r,t)$ is given by Equation 1. The solution to Equation 2 reveals the effective spot area is 26.7 cm^2 (5.8 cm diameter). The above formulation implicitly assumes the local mass-loss is linearly related to the heat flux. This approximation is not ideal given the extended tail of the distribution produced by Equation 1, biasing the large area of the outer annulus where the heat flux and mass loss are relatively small.

5. Conclusions

A series of high-heat-flux experiments were performed on a wide variety of materials examining their response to pulsed heat loads. At the highest fluence, 6,000 kJ/m^2, most of the materials responded dramatically with significant mass loss and charring. Mass-loss data were linear with fluence, although this trend was not explored for every material. The trends in mass-loss of the organics and polymers were self-similar, with a few exceptions (dry needles and PMMA). The net mass flux can be approximated using the mass loss and the calculated effective spot size (26.7 cm^2). These data contribute to the existing, mostly qualitative information on material response to nuclear weapons and other strong radiative heat sources.

6. Acknowledgements

The authors thank Bobby Thomas and Noah Siegel (USMC cadets) and Doug Robb for conducting the experiments at the solar furnace. Sandia is a multiprogram laboratory operated by Sandia Corporation, a Lockheed Martin Company, for the United States Department of Energy under Contract No. DE-AC04-94AL85000.

7. References

[1] B. Y. Lattimer, Heat fluxes from fires to surfaces, in: P.J. DiNenno, D. Drysdale, C.L. Beyler, W.D. Walton, R.L.P. Custer, J.R. Hall, J.M. Watts (Eds.), The SFPE Handbook of Fire Protection Engineering, National Fire Protection Association, Quincy, MA, 2002, pp. 2-269–2-296.

[2] S. Glasstone and P. J. Dolan, Thermal radiation and its effects, in: The Effects of Nuclear Weapons, US Department of Defense and US Department of Energy, 1977, pp. 276-323.

[3] S. B. Martin, Ignition of Organic Materials by Radiation, Fire Res. Abstr. Rev. 6 (1964) 85-98.

[4] S. B. Martin, Fire setting by nuclear explosion: A revisit and use in nonnuclear applications, J. of Fire Prot. Eng. 14 (2004) 283-297.

[5] S. B. Martin, Diffusion-controlled ignition of cellulosic materials by intense raidant energy, in Symp. (Int.) Combust. 10 (1965) 877-896.

[6] W. E. Strope and J. F. Christian, Fire aspects of civil defense, Fire Res. Abstr. Rev. 7 (1965) 155-166.

[7] C. K. Ho, S. S. Khalsa and N. P. Siegel, Analytical methods to evaluate flux distributions from point-focus collectors for solar furnace and dish engine applications, Proc. Int. Conf. on Energy Sustain. 4 (2010) 1-9.

[8] D. Drysdale, Steady burning of liquids and solids, in An Introduction to Fire Dynamics, John Wiley & Sons Ltd., Chichester, U.K., 1998, pp. 159–192.